EARTH SURFACE PROCESSES AND LANDFORMS
Earth Surf. Process. Landforms **39**, 1944–1959 (2014)

Published online 20 May 2014 in Wiley Online Library
(wileyonlinelibrary.com) DOI: 10.1002/esp.3589

Modelling particle residence times in agricultural river basins using a sediment budget model and fallout radionuclide tracers

Hugh G. Smith,[1]* William H. Blake[2] and Alex Taylor[2]
[1] School of Environmental Sciences, University of Liverpool, Liverpool, L697ZT, UK
[2] School of Geography, Earth and Environmental Sciences, Plymouth University, Plymouth, PL48AA, UK

Received 3 September 2013; Revised 14 April 2014; Accepted 15 April 2014

*Correspondence to: Hugh G. Smith, School of Environmental Sciences, University of Liverpool, Liverpool, L697ZT, UK. E-mail: hugh.smith@liverpool.ac.uk

ESPL
Earth Surface Processes and Landforms

ABSTRACT: Contemporary patterns in river basin sediment dynamics have been widely investigated but the timescales associated with current sediment delivery processes have received much less attention. Furthermore, no studies have quantified the effect of recent land use change on the residence or travel times of sediment transported through river basins. Such information is crucial for understanding contemporary river basin function and responses to natural and anthropogenic disturbances or management interventions. To address this need, we adopt a process-based modelling approach to quantify changes in spatial patterns and residence times of suspended sediment in response to recent agricultural land cover change. The sediment budget model SedNet was coupled with a mass balance model of particle residence times based on atmospheric and fluvial fluxes of three fallout radionuclide tracers (^{7}Be, excess ^{210}Pb and ^{137}Cs). Mean annual fluxes of suspended sediment were simulated in seven river basins (38–920 km^2) in south-west England for three land cover surveys (1990, 2000 and 2007). Suspended sediment flux increased across the basins from 0.5–15 to 1.4–37 kt y^{-1} in response to increasing arable land area between consecutive surveys. The residence time model divided basins into slow (upper surface soil) and rapid (river channel and connected hillslope sediment source area) transport compartments. Estimated theoretical residence times in the slow compartment decreased from 13–48 to 5.6–14 ky with the increase in basin sediment exports. In contrast, the short residence times for the rapid compartment increased from 185–256 to 260–368 d as the modelled connected source area expanded with increasing sediment supply from more arable land. The increase in sediment residence time was considered to correspond to longer sediment travel distances linked to larger connected source areas. This novel coupled modelling approach provides unique insight into river basin responses to recent environmental change not otherwise available from conventional measurement techniques. © 2014 The Authors. Earth Surface Processes and Landforms published by John Wiley & Sons Ltd.

KEYWORDS: sediment budgets; sediment residence time; connectivity; fallout radionuclides; river basins

Introduction

Quantifying the timescales of sediment transfer through river systems is fundamental for understanding river basin sediment and associated contaminant dynamics. This timescale is represented by the period of sediment residence or transit within a river basin that may encompass soil formation from bedrock, hillslope erosion and delivery to streams, storage and remobilization in channels and floodplains, and export from the basin outlet. Alternatively, sediment residence time may be determined for a subset of these components of the fluvial sediment cascade (Fryirs, 2013). Information on the residence time of sediment for different parts of a river basin is required to address research and river management questions of global importance. It has been used as a basis for interpreting the sedimentary response of river basins to changes in land cover and climate over the past 100 ky (Dosseto *et al.*, 2010). It can also be used to project timeframes for the removal of sediment-associated contaminants stored in river basins (Coulthard and Macklin, 2003; Malmon *et al.*, 2005), thereby providing valuable information to river managers.

Investigations of sediment residence time in river basins can be broadly divided into two categories, namely studies quantifying long-term weathering and denudation rates versus those focused on sediment dynamics in river channels and basins under recent environmental conditions. The first set of studies use cosmogenic or U-series isotopes to measure rates of sediment production from bedrock (Heimsath *et al.*, 2001; Fifield *et al.*, 2010) or sediment transit times through river basins over 1 to several 100 ky timescales (von Blanckenburg, 2005; Granet *et al.*, 2010). Studies in the second category quantify sediment transit over short hydrological timescales of more relevance to management. Such studies have used the fallout radionuclides ^{7}Be and excess ^{210}Pb (^{210}Pb$_{ex}$) to estimate fine sediment residence times or changes in sediment source in river channels spanning days to months (Bonniwell *et al.*, 1999; Matisoff *et al.*, 2005) and over decades (Wallbrink *et al.*, 1998, 2002; Gartner *et al.*, 2012). Fallout radionuclide tracers have also been used to estimate sediment residence times at the river basin scale (Dominik *et al.*, 1987; Le Cloarec *et al.*, 2007; Evrard *et al.*, 2010). Alternatively, the residence times of

sediment stored in floodplains have been estimated probabilistically from computations of sediment mass balances for reach-scale storage units (Dietrich and Dunne, 1978; Kelsey *et al.*, 1987; Malmon *et al.*, 2003).

The present study focuses on quantifying fine sediment residence times in river basins under recent environmental conditions. The objective was to model changes in spatial patterns and residence times of suspended sediment in response to contemporary agricultural land cover change. No studies have examined the effect of changes in land use on sediment residence time. While many previous studies have quantified the impact of land use change on the magnitude of sediment flux from catchments, changes to the timescales of sediment delivery in contemporary landscapes have been neglected. However, such information is crucial to the fundamental understanding of contemporary river basin sediment dynamics and the longer-term benefits, or otherwise, or sediment management measures. In this context, it also has important implications for residence times of sediment-associated contaminants. For example, changes to the duration of sediment storage in particular landscape compartments could affect the level of contaminant mobility with negative environmental consequences. Therefore, a new research focus is required to address this important knowledge gap.

Changes in sediment residence times in response to land cover change were, for the first time, modelled by combining a sediment budget model, SedNet, with a mass balance model of particle residence times based on three fallout radionuclide tracers, namely ^{7}Be, ^{210}Pb$_{ex}$ and ^{137}Cs. SedNet is a spatially-distributed model that represents erosion, sediment transfer and storage in steady state over a multi-decadal timescale (Prosser *et al.*, 2001a; Wilkinson *et al.*, 2004). It was developed in Australia and has been applied there to large river basins in tropical and temperate environments (McKergow *et al.*, 2005; Wilkinson *et al.*, 2009; Hughes and Croke, 2011). There have been no previous applications of SedNet to river basins in Europe or the UK.

Particle residence times were modelled using a mass balance approach based on atmospheric and fluvial fluxes of the fallout radionuclide tracers. The model was first proposed by Dominik *et al.* (1987) using only ^{7}Be and ^{210}Pb$_{ex}$. Subsequently, Le Cloarec *et al.* (2007) revised the model by including the ^{137}Cs soil inventory as an additional constraint. The model has been applied by Evrard *et al.* (2010) to investigate sediment dynamics in several small catchments in the tropical highlands of Mexico. In contrast, the present study differs from previous applications of the residence time model by employing multi-decadal estimates of fallout and fluvial export. Previous applications were based on short-term monitoring (1–2 years) that is highly dependent on the specific hydroclimatic conditions during measurement periods. Furthermore, these studies did not address changes in residence times in response to land cover change, which requires a dedicated model-based approach. The present study focuses on simulating residence times in seven river basins (38–920 km^2) situated in south-west England for land covers corresponding to three surveys produced from satellite imagery between 1990 and 2007.

Methods

River basins

Modelling and field measurements were undertaken in seven agricultural river basins located in south-west England (Figure 1). Six of the basins are nested within the River Tamar basin upstream of the village of Gunnislake (920 km^2) and include the Rivers Carey (67 km^2), Inny (97 km^2), Kensey (38 km^2), Lyd (219 km^2), Ottery (124 km^2), and a second measurement site on the main channel of the Tamar in the upper basin (Tamar Upper; 238 km^2). The River Tamar forms the main boundary between the counties of Devon and Cornwall and drains south into the Tamar Estuary at Plymouth. All measurements and modelling

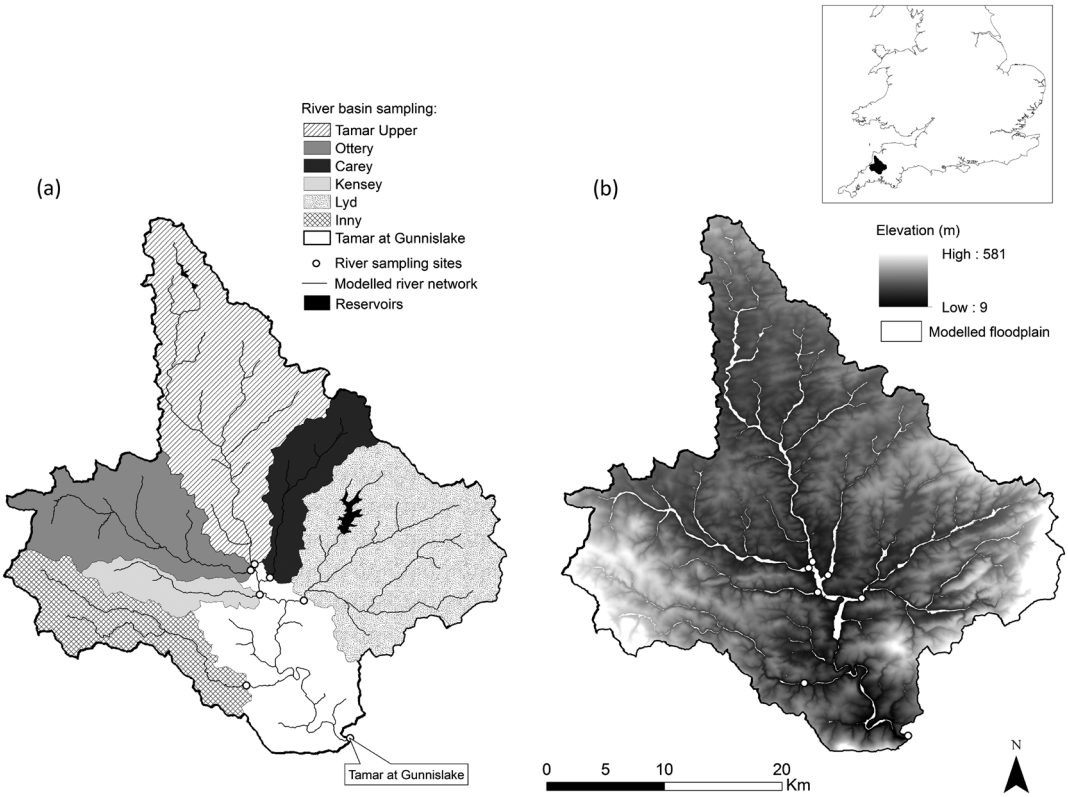

Figure 1. River Tamar study basin showing (a) the monitored sub-basins with the modelled channel network and (b) digital elevation model (10 m grid size) and the modelled floodplain.

were undertaken upstream of the tidal limit. The topography is characterized by short, steep hillslopes in the lower and mid Tamar basin, with lower relief terrain in the upper basin. Maximum elevations (up to 581 m) occur in the small areas of granitic moorland to the east and west.

Most of the basins are underlain by fine sedimentary rocks (mudstones, shales and sandstones). Soils are predominantly loamy, with some peaty soils in upland areas. The extent of floodplain is limited and confined by narrow steep-sided valleys and shallow bedrock. The largest floodplain area is located in the middle of the main Tamar basin. The section of main channel between the Inny and the basin outlet at Gunnislake is extensively bedrock confined. Land cover is mostly agricultural (grassland and arable) with a small area of woodland (<16%). Surveys of land cover based on satellite imagery were completed in 1990, 2000 and 2007 (Morton *et al.*, 2011).

Precipitation across the study basins falls predominantly as rain and exhibits pronounced spatial variability with the highest annual totals occurring over the upland areas to the east and west. Across the Tamar basin, mean annual precipitation was 1284 mm based on 1 × 1 km gridded data for 1971 to 2000. The mean daily river flow measured at Gunnislake was 22.4 $m^3\ s^{-1}$ and ranged between 0.58 and 482 $m^3\ s^{-1}$ for the period from 1956 to 2012. There is also pronounced seasonality in rainfall and river flows, with the highest discharge generally occurring from November to March in association with Atlantic cold fronts.

Field measurements and laboratory analysis

Suspended sediment samples were collected continuously at the outlets of each river basin over a 12 month period. *In situ* time-integrated samplers based on the design by Phillips *et al.* (2000) were deployed in pairs at riffles. The samplers were made from polyvinylchloride (PVC) tubes 1 m in length and 0.11 m in diameter with sealed caps at both ends that contained 3 mm diameter inlet and outlet tubes. Water and suspended sediment pass through the narrow inlet tube and enter the PVC tube where the change in cross-sectional area promotes a reduction in flow velocity and sedimentation (Phillips *et al.*, 2000). Under some conditions, these samplers may under-sample the very fine fraction (<2 μm) of suspended material, although Phillips *et al.* (2000) noted that the transport of very fine particles as aggregates should reduce the level of under-sampling that was observed during laboratory experiments. Samples were collected at approximately monthly intervals from September 2011 to October 2012. During this time the mean daily flow for the River Tamar at Gunnislake was slightly above average at 23.9 $m^3\ s^{-1}$ and ranged between 4.5 and 155 $m^3\ s^{-1}$.

All sediment samples were analysed for the three fallout radionuclides following freeze-drying and gentle disaggregation. Samples were sealed for 21 days in either 50 mm Petri dishes or in 4 mm vials for some low mass samples to allow equilibration between ^{214}Pb and its parent ^{226}Ra. Activity concentrations of the radionuclides were measured using low background EGandG Ortec planar (GMX50-83-LB-C-SMN-S) and well (GWL-170-15-S) HPGe gamma spectrometers at the Plymouth University Consolidated Radio-isotope Facility within an ISO 9001:2008-certified framework. $^{210}Pb_{ex}$ was determined by subtraction of ^{226}Ra activity measured using ^{214}Pb gamma emissions (295 and 352 keV) from total ^{210}Pb (46.5 keV). ^{137}Cs and ^{7}Be activities were determined from gamma emissions at 662 and 478 keV, respectively. Detector efficiency for ^{7}Be was determined by interpolation between the efficiency values of ^{137}Cs (662 keV) and ^{113}Sn (392 keV). Count times were typically 86 ks, although some low mass sediment samples were counted for 172 ks. Sample calibration was carried out using standards of the same geometry and matrix as the experimental samples. Standards were prepared using a mixed standard solution (G E Healthcare, Amersham, UK) which was distributed in a sediment matrix. Sample counts were corrected for background emission, geometry efficiency and decay. All values were decay corrected to the time of sampling and reported as activity concentration (Bq kg^{-1}). Analytical performance was assessed by inter-laboratory comparison tests using materials supplied by the International Atomic Energy Agency.

Sediment budget model

SedNet derives a river network from a Digital Elevation Model (DEM). This network is divided into river links that are formed between adjacent stream junctions and includes the internal contributing area draining into each link. The mean annual suspended sediment mass balance (t y^{-1}) is computed for each river link from internal hillslope, gully and riverbank erosion and upstream tributary inputs less floodplain and reservoir deposition losses. The net flux of suspended sediment is passed to the next downstream link. Transient storage of suspended sediment within the channel network is neglected because this is considered small relative to total yields over multi-decadal timescales (Wilkinson *et al.*, 2009).

Hillslope soil erosion is modelled using a spatially-distributed version of the Revised Universal Soil Loss Equation (RUSLE, Renard *et al.*, 1997). RUSLE is used to predict mean annual soil loss (A, t $ha^{-1}\ y^{-1}$) from rill and interrill erosion based on the product of six empirically-derived factors:

$$A = RKLSCP \quad (1)$$

These are rainfall erosivity (R), soil erodibility (K), slope length (L) and steepness (S), cover (C) and management practice (P). The procedures for calculating each RUSLE factor are outlined in Table I. In the absence of specific information about management practices across the study basins, P was not explicitly included in the computation of A (i.e. it was set to 1). SedNet does not include representation of small-scale features such as roads, tracks or ditches that may either generate sediment or act as transport pathways. The RUSLE factors were produced as a set of raster grids with three grids for C factors corresponding to the 1990, 2000 and 2007 land cover surveys.

The proportion of sediment from hillslope erosion delivered to the river network was represented using a hillslope sediment delivery ratio (*HSDR*). This is designed to account for the discrepancy between plot-scale erosion rates and small basin sediment yields, reflecting short sediment travel distances on hillslopes (Parsons *et al.*, 2006) and storage opportunities (e.g. farm dams, contour banks) between slopes and the channel network (Prosser *et al.*, 2001b; Slattery *et al.*, 2002). At larger basin scales, it is not practical to capture the small scale variability in *HSDR*. Therefore, the *HSDR* was set to 0.15 in the present study in accordance with field measurements made by Walling *et al.* (2002) in small agricultural basins (<4 km^2) in central England. The mean annual supply of hillslope-derived sediment (HS_x, t y^{-1}) to the modelled channel network in each river link is determined by $HS_x = HSDR\sum_{j=1}^{j=n} A_j$, where A_j is the mean annual RUSLE erosion rate calculated for each grid cell j in the internal drainage area containing n cells for each river link x.

Gully erosion was not observed in the study basins and this component of SedNet was not used. Riverbank erosion for each

Table I. Summary of data inputs and processing for calculation of the RUSLE factors for use in the SedNet model

RUSLE factor	Data input and source	Data processing
Rainfall erosivity (*R*)	Plymouth University, Princetown and St Mawgan (12–15 years) sub-hourly rainfall records; British Atmospheric Data Centre, Plymouth University and the UK Met Office	Rainfall erosivity (*R*, MJ mm ha^{-1} h^{-1} y^{-1}) was calculated using the kinetic energy relationship of Marshall and Palmer (1948) recommended for the UK by Morgan (2001): $KE = 0.0895 + 0.0844 log_{10}(I)$ where *KE* is kinetic energy per unit rainfall (MJ ha^{-1} mm^{-1}) and *I* is rainfall intensity (mm h^{-1}). EI_{30} was calculated for each event as the product of total kinetic energy (*E*, MJ ha^{-1}) and the maximum 30-min rainfall intensity (I_{30} , mm h^{-1}). The linear regression $R = 1.3723A - 551.27$ ($R^2 = 0.95$) between the annual sum of EI_{30} (*R*) and annual rainfall (*A*, mm y^{-1}) for data from the three rain gauges was used to calculate gridded *R* values using the 1 × 1 km grid of 30-year mean annual precipitation (1971–2000) for the river basins.
Soil erodibility (*K*)	Digital soil vector map and soil attribute data; National Soil Resources Institute, Cranfield University[a]	Soil erodibility (K, t ha h ha^{-1} MJ^{-1} mm^{-1}) was calculated according to Wischmeier and Smith (1978): $K = \frac{2.1 \times 10^{-4}(12-OM)M^{1.14} + 3.25(S-2) + 2.5(P-3)}{7.59 \times 100}$ where *OM* is soil organic matter content (%), *M* = (%silt + %very fine sand) x (100 - %clay), *S* is the soil structure class and *P* is the permeability class.
Slope length (*L*)	10 m DEM UK Ordnance Survey	Slope length (*L*) was calculated on the basis of contributing areas according to Desmet and Govers (1996): $L_{i,j} = \frac{\left(A_{i,j,in} + D^2\right)^{m+1} - A_{i,j,in}^{m+1}}{D^{m+2} x_{i,j}^{m} (22.13)^{m}}$ where $A_{i,j,in}$ is the contributing area (m^2) to the grid cell with coordinates (i,j), D is the grid cell size (10 m), $x_{i,j} = \sin\alpha_{i,j} + \cos\alpha_{i,j}$ where $\alpha_{i,j}$ is the aspect direction for the grid cell with coordinates (*i*,*j*), *m* is a variable slope length exponent related to the ratio ε of rill to interrill erosion by $m = \varepsilon/(1 + \varepsilon)$ in which ε is calculated for soil that is moderately susceptible to both rill and interill erosion by $\varepsilon = \sin\theta/(0.0896[3.0(\sin\theta)^{0.8} + 0.56])$, where θ is the slope angle (*Renard et al.*, 1997). In the present study, the maximum slope length was limited to 300 m to reduce the likelihood of channel formation with increasing contributing area (Renard *et al.*, 1997).
Slope steepness (*S*)	10 m DEM UK Ordnance Survey	Slope steepness (*S*) was calculated using the equation recommended by McCool *et al.* (1987) where θ is slope angle: $S = \begin{cases} 10.8\ sin\theta + 0.03, & s < 9\% \\ 16.8\ sin\theta - 0.50, & s \geq 9\% \end{cases}$
Cover (*C*)	UK land cover surveys for 1990, 2000 and 2007 (25 m raster grids). Centre for Ecology and Hydrology	Cover (*C*) values were based on the range of values estimated by Morgan (2005); Fu *et al.* (2006); Van Rompaey and Govers (2002) and Wischmeier and Smith (1978): Arable land *C* = 0.25; pasture *C* = 0.01; forest *C* = 0.001; shrub/heath *C* = 0.01; urban and inland bare ground *C* = 0.03.

[a]Soils data © Cranfield University (NSRI) and for the Controller of HMSO 2012

river link (BE_x, t y^{-1}) is modelled by relating link stream power ($pgQ_{bf}S_x$) to bank erodibility (Wilkinson *et al.*, 2005), which is represented as a function of riparian vegetation and floodplain width, as in the following equation:

$$BE_x = c\rho g Q_{bf} S_x (1 - PR_x)\left[1 - e^{-0.008F_x}\right](L_x h \rho_s p_s) \quad (2)$$

where c is a coefficient that is set to limit the maximum bank retreat rate ($c = 0.0001$), ρ is the density of water, g is acceleration due to gravity, Q_{bf} is bankfull discharge (m^3 s^{-1}), S_x is the energy slope approximated by channel gradient, PR is the proportion of intact riparian vegetation along a river link (defined here as forest or woodland cover in 1× 25 m cell either side of the modelled channel network), F_x is floodplain width (calculated as floodplain area divided by river link length), L_x is the link length (m), h is mean bank height (0.93 m), ρ_s is soil bulk density (1.5 t m^{-3} for the full bank profile) and p_s is the proportional bank contribution of fine sediment to suspended load (Table II). Bankfull discharge was defined as the flow with a recurrence interval of 1.5 years on the annual series based on a survey of UK rivers (Davidson and Hey, 2011). The increasing proportion of riparian forest or woodland along a river link was considered to reduce bank erodibility through the effect of tree root reinforcement increasing bank stability (Thorne, 1990; Abernethy and Rutherfurd, 2001). Floodplain width was used as a surrogate for exposure to bedrock such that there was an exponential decline in bank erodibility with decreasing floodplain width corresponding to increased bedrock exposure (Wilkinson *et al.*, 2005).

Floodplain deposition (FD_x, t y^{-1}) is computed as a function of floodplain area and the median value of daily overbank flow (Prosser *et al.*, 2001b):

$$FD_x = \frac{Q_f}{Q}(I_x)\left(1 - e^{-\left(\frac{vA_f}{Q_f}\right)}\right) \quad (3)$$

where Q_f is the median of the set of daily overbank discharges determined from the amount by which total daily discharge (Q) exceeds bankfull discharge (Q_{bf}), I_x is the total suspended sediment supply to the link x, A_f is the floodplain area and v is the particle settling velocity (1×10^{-6} m s^{-1}) based on Stokes Law for particles with diameters 1–4 μm such that that larger particles can be expected to have settled during the period of overbank flow (Wilkinson *et al.*, 2009). It is assumed that the proportion of sediment delivered to the floodplain equates to the proportion of discharge that goes overbank relative to total discharge. The floodplain extent was defined by the Multi-Resolution Valley Bottom Flatness (MRVBF) terrain index developed by Gallant and Dowling (2003). Reservoir deposition is calculated as a function of the mean annual reservoir inflow and its total storage capacity based on a revised version of the Brune Rule that is used to determine sediment trapping efficiency (Brune, 1953; Heinemann, 1981).

Hydrological regionalization is required to provide estimates of mean annual discharge (*MAD*), bankfull discharge (Q_{bf}), and median overbank discharge (Q_f) for each river link for use in erosion and deposition modelling. This is based on long-term gauge records of unregulated discharge (Table II) for which *MAD*, Q_{bf} and Q_f were calculated. The runoff coefficient (R_c) is estimated by combining a simplified water balance where $R_c = (P - E)/P$ with a rational function relating mean annual precipitation (P), evapotranspiration (E) and potential evaporation (E_0) (Zhang *et al.*, 2004), to give Equation (4) (Wilkinson *et al.*, 2006):

Table II. Summary of SedNet model data inputs and parameter values

Model input	Datasets and parameters	Data source
Topography	10 m DEM	UK Ordnance Survey
Floodplain extent	MRVBF index > 3.5 clipped by 100 year recurrence interval flood extent	100 year flood layer: UK Environment Agency
Mean annual precipitation	1 × 1 km grid of 30 year mean annual precipitation (1971–2000)	UK Met Office
Potential evaporation	MORECS 40 × 40 km grid	UK Met Office
River flow	Unregulated flow: 5 river gauges (18–26 years); Regulated flow: 6 river gauges (22–37 years)	UK Environment Agency/ Centre for Ecology and Hydrology
Bankfull recurrence interval	1.5 years on the annual maximum series	Davidson and Hey (2011)
Mean bank height (H)	H = 0.93 ± 0.22 m	Channel network survey (n = 20 sites)
Channel width (W)-catchment area (A)	$W = 1.346A^{0.4885}$ ($R^2 = 0.94$)	Channel network survey (n = 20 sites)
Proportion fine vs. coarse sediment (bank erosion)	0.74 vs. 0.26: Mean clay, silt and very fine sand vs. remaining sand content for riparian soils. The mean fraction of sampled suspended material < 63μm was 0.89 ± 0.06.	Digital soil map; National Soil Resources Institute, Cranfield University[a]
Riparian vegetation (bank erosion)	Clipped 25 m buffer either side of modelled channel network for 1990, 2000 and 2007 land cover surveys	UK Centre for Ecology and Hydrology
Hillslope sediment delivery ratio (HSDR)	0.15	Walling *et al.* (2002)

[a]Soils data © Cranfield University (NSRI) and for the Controller of HMSO 2012.

$$R_c = \left[1 + \left(\frac{E_0}{P}\right)^{(a(E_0/P)+b)}\right]^{1/(a(E_0/P)+b)} - \frac{E_0}{P} \quad (4)$$

The parameters a and b are fitted by least squares regression for E_0/P versus R_c for the gauged river basins. R_c was estimated for all river links based on the mean of the gridded E_0/P for each link and then used to calculate MAD for all links, where $MAD = R_c P A$ and A is the internal drainage area for each link. Q_{bf} and Q_f are regionalized as a function of MAD using gauge data where $Q_{bf} = g(MAD)^h$ and $Q_f = j(MAD)^k$ and g, h, j and k are fitted parameters (Wilkinson *et al.*, 2004). Flow in the Tamar basin is affected by the operation of Roadford Reservoir (built 1989; capacity 34.5 GL) in the Lyd sub-basin and to a lesser extent the Upper Tamar Lake (built 1975; capacity 1.48 GL) in the north (Figure 1(a)). River gauge data available for the period following reservoir construction (Table II) was used to adjust the regionalized MAD for river links affected by reservoir diversions and this change was propagated to downstream links.

Radionuclide residence time model

The residence time model computes radionuclide mass balances using basin inputs and fluvial export of ^{7}Be, ^{210}Pb$_{ex}$ and ^{137}Cs for river basins divided into slow and rapid transport compartments. The compartments are defined according to transport velocity (Dominik *et al.*, 1987). The slow compartment represents the upper soil profile containing the fallout radionuclide inventories (<0.30 m soil depth). It is characterized by long residence times that correspond to the period of storage and transfer of radionuclides from the upper soil profile to the rapid compartment. The rapid compartment represents river and reservoir surfaces as well as the immediate surroundings that have much shorter radionuclide residence times. This includes runoff and sediment-generating areas on hillslopes that are connected to the river network. Rapid compartment residence times were considered to represent the mobilization and transfer of radionuclides from connected source areas to the basin outlets over approximately seasonal to annual timescales. Model estimates of residence times should be interpreted as mean values under steady state conditions for each land cover.

The fallout radionuclides employed here have been widely used as soil erosion and sediment source tracers (see reviews by Wallbrink and Murray, 1993; Walling, 2003; Mabit *et al.*, 2008; Taylor *et al.*, 2013). ^{7}Be ($t_{1/2}$ = 53 days) is a naturally occurring radionuclide produced by cosmic ray spallation of nitrogen and oxygen in the upper atmosphere. Fallout occurs predominantly in association with precipitation (Wallbrink and Murray, 1994). ^{210}Pb$_{ex}$ ($t_{1/2}$ = 22 years) refers to the amount of ^{210}Pb derived from atmospheric fallout that exceeds that supported by decay of its lithogenic parent ^{226}Ra *in situ*. ^{137}Cs ($t_{1/2}$ = 30 years) was produced by atmospheric nuclear weapons testing during the 1950–1960s and dispersed globally, with subsequent less extensive releases from the Chernobyl and Fukushima nuclear power plant accidents. The main basis for use of these fallout radionuclides as sediment tracers is their tendency to strongly adsorb to fine particles (Cremers *et al.*, 1988; He and Walling, 1996). This is reflected in the high partition coefficients (K_d). In the present study, K_d values of 1.0×10^5, 1.0×10^6 and 8.4×10^4 L kg^{-1} for freshwater conditions were used for ^{7}Be, ^{210}Pb$_{ex}$ and ^{137}Cs, respectively, based on the summary of values presented by Le Cloarec *et al.* (2007). Use of these values assumes that environmental conditions which may affect radionuclide mobility between the particulate and dissolved phases remain unchanged across the study basins (Taylor *et al.*, 2012).

The model requires estimates for the atmospheric input of ^{7}Be and ^{210}Pb$_{ex}$, the soil inventory of ^{137}Cs (since fallout is now negligible) and fluvial export of particulate and dissolved fractions. Atmospheric fallout was estimated using mean annual rainwater concentrations for ^{7}Be and ^{210}Pb$_{ex}$ of 1.97 ± 0.3 Bq L^{-1} (Taylor, 2012) and 0.1 ± 0.008 Bq L^{-1} (Peirson *et al.*, 1966), respectively. ^{7}Be in rainwater was measured south of the Tamar basin at Plymouth during 2009-2010, while ^{210}Pb$_{ex}$ was measured between 1962 and 1964 at Milford Haven in south Wales. Mean annual rainwater concentrations were combined with 1 × 1 km gridded data for 1971–2000 mean annual precipitation to compute mean annual fallout for each river basin (Table III). The ^{137}Cs soil inventory (I_{Cs}, Bq m^{-2}) was estimated using the regression relationship $I_{Cs} = 4.16R + 1400$, where R is mean annual rainfall. This was derived by Appleby *et al.* (2003) using soil inventory data (to 0.3 m depth) from locations across Great Britain that were sampled in 1977 (Cawse, 1983). This relationship was applied to the gridded mean annual precipitation data to estimate the ^{137}Cs inventory for each river basin, which was corrected for radioactive decay to 2012. There was negligible fallout from the 1986 Chernobyl nuclear accident in south-west England (Walling *et al.*, 1989).

The proportional contribution of sediment from hillslope surface and channel bank erosion affects the activity concentrations of fallout radionuclides in suspended sediment (Wallbrink *et al.*, 2003; Smith *et al.*, 2011). This reflects the soil profile distribution of the radionuclides, where maximum concentrations occur at or near the surface and decrease exponentially with depth to negligible levels (Wallbrink *et al.*, 1999). Therefore, the effect of changes in modelled hillslope and channel bank sediment contributions on radionuclide activity concentrations required consideration. The measured activity concentrations (Table III) were considered closest to values for suspended sediment exported under 2007 land cover because of a consistent trend of increasing arable land from 1990 to 2007 that increased modelled hillslope sediment contributions. Suspended sediment activity concentrations for the 1990 and 2000 simulations were scaled by the modelled proportion of hillslope sediment supply (HS) relative to total supply (TS) for each river basin. This ratio was then divided by the equivalent ratio for 2007 and multiplied by the measured activity concentrations for each radionuclide (C_m) to give the estimated concentrations (C_{et}) for survey years t (1990, 2000):

$$C_{et} = C_m\left((HS/TS)_t/(HS/TS)_{07}\right) \quad (5)$$

Fluvial export of radionuclides associated with suspended sediment was calculated by multiplying the estimated (1990, 2000) or measured (approximating 2007) concentrations with the respective modelled mean annual suspended sediment output for each river basin. The factor changes in estimated activity concentrations for 1990 and 2000 compared with measured values equated to 0.62–0.78 and 0.91–0.98, respectively. The effect of earlier radionuclide activity concentrations on subsequent estimates for suspended sediment were considered minimal because of the frequency of higher magnitude flows that could be expected to remove fine sediment from storage within the channel network over approximately seasonal to annual timescales. The dissolved radionuclide flux (F_d) was determined using the literature-based K_d values for fresh water with activity concentrations for suspended sediment (C) and regionalized mean annual discharge (MAD) for each river basin (where $F_d = C(1/K_d)MAD$).

The residence time model requires solutions to four Equations (6)-(9). The fraction of the basin area represented

Table III. Study basin characteristics, estimated fallout and mean activity concentrations obtained from time-integrated suspended sediment sampling

River basins	Basin area (km^2)	Mean annual precipitation, MAP (mm)	Modelled mean annual discharge, MAD (mm)	Relief ratio, RR[a]	Normalised MAD.RR[b]	Estimated mean fallout, F_a ($MBq\ y^{-1}$)			Mean suspended sediment activity concentration ± SE ($Bq\ kg^{-1}$)[d]		
						^{7}Be ($\times 10^5$)	$^{210}Pb_{ex}$ ($\times 10^5$)	^{137}Cs, M (MBq, $\times 10^5$)[c]	^{7}Be[e]	$^{210}Pb_{ex}$	^{137}Cs
Tamar Upper	238	1214	658	0.006	0.12	5.7	0.29	6.9	127 ± 13	42.1 ± 2.9	4.8 ± 0.9
Ottery	124	1255	740	0.011	0.27	3.1	0.16	3.7	131 ± 13	47.0 ± 5.8	4.6 ± 0.9
Carey	67	1180	669	0.011	0.24	1.6	0.08	1.9	113 ± 11	48.4 ± 4.5	5.9 ± 0.7
Kensey	38	1333	832	0.014	0.39	0.99	0.05	1.2	255 ± 21	104 ± 8.3	8.3 ± 0.9
Lyd	219	1325	733	0.029	0.69	5.7	0.29	6.8	152 ± 25	60.6 ± 12	10 ± 1.3
Inny	97	1488	1070	0.014	0.49	2.8	0.14	3.3	207 ± 13	91.5 ± 5.9	8.5 ± 0.4
Tamar Gunnislake	920	1284	750	0.012	0.30	23	1.2	28	166 ± 14	53.8 ± 3.5	6.6 ± 0.2

[a]Relief ratio is a measure of basin slope and is defined as the maximum basin relief divided by the maximum horizontal length measured parallel to the main river channel.
[b]MAD and RR were normalised by dividing by their respective maximum values and then multiplied (range 0–1).
[c]For ^{137}Cs, the estimated total fallout inventory (M) for each basin was based on a relationship between soil inventory and mean annual rainfall (Appleby *et al.*, 2003).
[d]Mean suspended sediment activity concentrations were calculated from measurements of 12 monthly time-integrated suspended sediment samples (with 10 monthly samples for the River Carey).
[e]Mean monthly measured ^{7}Be activity concentrations were decay-corrected by apportioning activity according to the daily proportional flow during each month and then correcting for the number of days until the sampling date. Flow was used as a surrogate for daily suspended sediment and associated ^{7}Be input to the samplers. $^{210}Pb_{ex}$ and ^{137}Cs were decay-corrected to the sampling date.

by the slow (S_s) and rapid (S_r) transport compartments is used to partition atmospheric fallout (Equation (6)):

$$S_s + S_r = 1 \tag{6}$$

The mass balance for the slow compartment is represented by input from atmospheric fallout (F_a) with losses from the soil radionuclide inventory (I_s) dependent on the rate of transport out of the slow compartment (k_s) and radioactive decay (λ):

$$F_a S_s = I_s(k_s + \lambda) \tag{7}$$

The transport rate out of the slow compartment is related to the residence time (τ_s) by $k_s = 1/\tau_s$. For the rapid compartment, atmospheric input is added to the flux from the slow compartment which is balanced by losses due to fluvial export or radioactive decay:

$$F_a S_r + I_s k_s = I_r(k_r + \lambda) \tag{8}$$

where I_r is the radionuclide inventory in the rapid compartment and k_r is the rate of export from the rapid compartment. The fluvial export of radionuclides from the river basin (F_r) is calculated as

$$F_r = I_r k_r \tag{9}$$

Solutions to Equations (6–9) for the unknown variables S_r, k_s, k_r, I_s and I_r can be obtained using estimates of atmospheric fallout, soil inventory (^{137}Cs only) and fluvial export for all three fallout radionuclides (Dominik *et al.*, 1987; Le Cloarec *et al.*, 2007). However, these solutions require several assumptions. The first is that most ^{7}Be in the slow compartment will be lost to radioactive decay rather than be exported from this compartment given its short half-life of 53 d (i.e. $k_s \ll \lambda_{Be}$). Export from the slow to the rapid compartment is considered negligible compared to atmospheric fallout to the rapid compartment (i.e. $k_s(I_s)_{Be} \ll S_r(F_a)_{Be}$). It is also assumed that the duration of sediment storage in the rapid compartment does not result in net decay of ^{7}Be to levels below the limit of detection. Furthermore, the decay rate of $^{210}Pb_{ex}$ is considered negligible compared to the export rate from the rapid compartment (i.e. $\lambda_{Pb} \ll k_r$).

The rapid compartment area (S_r) can be determined by combining Equations (8) and (9) based on the first assumption such that S_r is a function of the ratio F_r/F_a for ^{7}Be and the export rate ($k_r = 1/\tau_r$):

$$S_r = \left(\frac{F_r}{F_a}\right)_{Be}\left(\frac{\lambda_{Be}}{k_r} + 1\right) \tag{10}$$

The slow compartment residence time (τ_s) is then computed by solving Equations (6)-(9) for $^{210}Pb_{ex}$ with the assumption that $\lambda_{Pb} \ll k_r$ and combining this with Equation (10):

$$\tau_s = \frac{\left(\frac{1}{\lambda_{Pb}}\right)\left[1 - \left(\frac{F_a}{F_r}\right)_{Pb}\right]}{\left(\frac{R_r}{R_a}\right)(1 + \lambda_{Be}\tau_r) - 1} \tag{11}$$

where $R_r = (F_r)_{Be}/(F_r)_{Pb}$ and $R_a = (F_a)_{Be}/(F_a)_{Pb}$.

Slow compartment residence time can also be calculated using the mass balance equations for ^{137}Cs with basin-scale inventory (M) rather than fallout (Le Cloarec *et al.*, 2007) to give:

$$\tau_s = \frac{\left[M - (F_r)_{Cs}\tau_r\right]}{(F_r)_{Cs}(\lambda_{Cs}\tau_r + 1)} \tag{12}$$

where $M = (I_s)_{Cs} + (I_r)_{Cs}$

The rapid compartment residence time (τ_r) may then be obtained by combining Equations (11) and (12) and finding a

solution to the equation:

$$a(\tau_r)^2 + b(\tau_r) + c = 0 \quad (13)$$

where

$$a = -(F_r)_{Cs}\left(\frac{R_r}{R_a}\right)\lambda_{Be}\lambda_{Pb}$$

$$b = M\left(\frac{R_r}{R_a}\right)\lambda_{Be}\lambda_{Pb} - (F_r)_{Cs}\lambda_{Pb}\left(\frac{R_r}{R_a} - 1\right) - (F_r)_{Cs}A\lambda_{Cs}$$

$$c = \lambda_{Pb}M\left(\frac{R_r}{R_a} - 1\right) - A(F_r)_{Cs}$$

in which

$$A = 1 - \left(\frac{F_a}{F_r}\right)_{Pb}$$

A sensitivity analysis similar to that employed by Le Cloarec *et al*. (2007) was used to determine the effect of changes in input parameter values on τ_s, τ_r and S_r. Factor changes of 0.5 and 1.5 were applied to suspended sediment flux (*SS*), F_a ($^{210}Pb_{ex}$), F_a (^{7}Be) and M (^{137}Cs) for the Tamar basin upstream of Gunnislake under 2007 land cover. Changes in model outputs that resulted from effectively ignoring K_d (set to 1×10^{12} L kg^{-1}) as well as varying radionuclide activity concentrations by ± 2 standard errors were also examined. Factor changes in model outputs were determined by the equation:

$$FC = 1 + \frac{(O_v - O_i)}{O_i} \quad (14)$$

where *FC* is the factor change in model outputs (*O*) resulting from the relative difference between outputs based on varied parameter values (O_v) and initial parameter values (O_i).

Results and Discussion

Sediment budgets and land cover change

Suspended sediment budgets were modelled for the entire Tamar River basin for land covers corresponding to the 1990, 2000 and 2007 surveys. These basin-wide budgets show a large increase in hillslope sediment contributions between 1990 and 2007 in response to an increasing proportion of arable land (Table IV). The mean annual hillslope sediment contribution range for 1990–2007 was 8.8–32 kt y^{-1} with an *HSDR* of 0.15. The bank erosion contribution to suspended sediment was between 7.7 and 8.4 kt y^{-1}. Total sediment storage in reservoirs and floodplains was minor (1.3–3.6 kt y^{-1}) resulting in mean annual basin suspended sediment exports of 15–37 kt y^{-1}, which equated to a range in yields of 16–40 t km^{-2} y^{-1} based on the *HSDR* of 0.15. The increase in river link ($n = 92$) suspended sediment flux between consecutive land cover surveys was distributed across the Tamar basin (Figure 2).

Table IV. Summary of suspended sediment budgets for the River Tamar basin upstream of Gunnislake for three land covers and two *HSDR* values

Land cover survey	Arable land area (%)	*HSDR*	Inputs (kt y^{-1})		Outputs (kt y^{-1})			
			Hillslope	Channel banks	Reservoir	Floodplain	Basin export	Basin yield (t km^{-2} y^{-1})
1990	6.3	0.05	2.9	7.7	0.15	0.6	9.9	11
2000	22	0.05	7.8	7.7	0.23	0.8	14	16
2007	36	0.05	11	8.4	0.40	1.1	18	19
1990	6.3	0.15	8.8	7.7	0.42	0.9	15	16
2000	22	0.15	23	7.7	0.67	1.7	29	31
2007	36	0.15	32	8.4	1.2	2.4	37	40

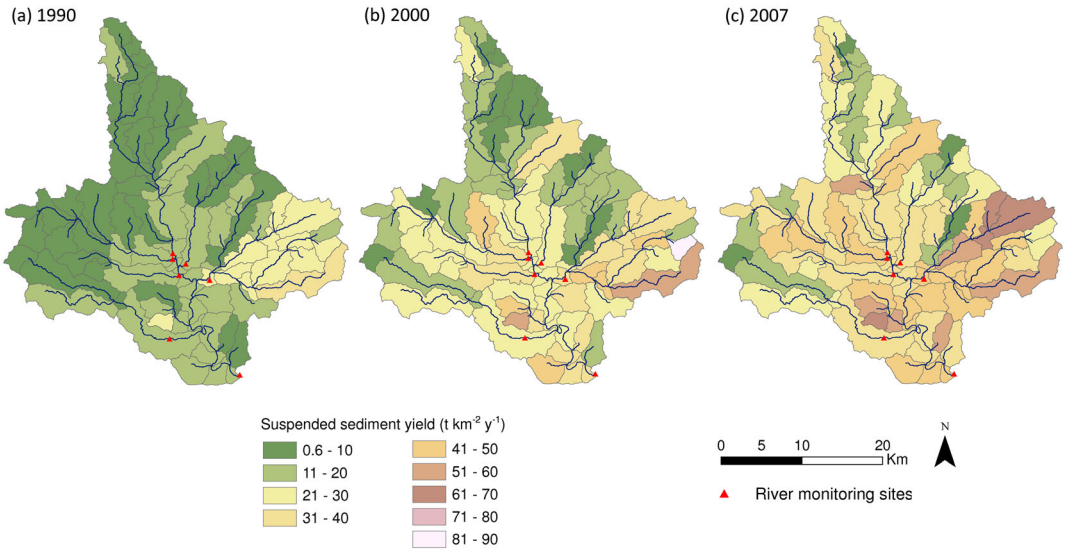

Figure 2. Modelled suspended sediment yields for each river link ($n = 92$) for the (a) 1990, (b) 2000 and (c) 2007 land covers with *HSDR* = 0.15 for the River Tamar basin upstream of Gunnislake. This figure is available in colour online at wileyonlinelibrary.com/journal/esp

The highest modelled fluxes occurred in the headwaters of the River Lyd sub-basin (Figure 1(a)), which was characterized by the highest rainfall erosivity, local slope gradients and basin relief ratio values.

Uncertainty in change detection between land cover surveys represents an important challenge in the use of remotely sensed datasets (Fuller *et al.*, 2003). Accuracy in the detection of land cover changes is of less concern if the focus of modelling were to use only these data to characterize land cover scenarios for modelling. However, accurate detection of land cover changes during the survey period (1990–2007) is important if model outputs are to be interpreted as a meaningful representation of the effects of recent change. The large increase in arable land cover (6.3 to 36%) represented the main change during the survey period. It was mostly offset by a reduction in the areas classified as grassland. Other land uses such as forest/woodland (11–16%), urban (1–3%) and shrub/heath/bog (all 1%) were reasonably consistent between surveys.

The trend of increasing arable land cover for the Tamar basin can be assessed by comparison with land use data from county-scale farm surveys for Devon and Cornwall (Department of Environment, Food and Rural Affairs (DEFRA), 2010). Between the 1995 and 2005 surveys, there was an 8% and 6% increase in cropped land area in Devon and Cornwall, respectively. Interpolating between farm survey years suggests an increase of 13% and 24% for Devon and Cornwall from 1990 to 2007 compared with 30% for the Tamar basin. There was also a consistent trend of increasing arable land area between consecutive farm surveys spanning the full land cover survey period (1985–2009). This provides increased confidence in the changes in arable land cover recorded in the Tamar basin by satellite imagery. It also indicates that model simulations are relevant for understanding the effect of recent land cover changes on erosion and sediment transfer.

Particle residence times

Modelled slow compartment residence times for the river basins were 13–48, 7.7–17 and 5.6–14 ky for the 1990, 2000 and 2007 land covers, respectively (Table V). The decline in the theoretical mean residence times of radionuclides in the upper soil profile was related to the increase in arable land area and associated increase in modelled suspended sediment exports with consecutive land cover surveys (Table V). Between 1990 and 2007, arable land cover in the river basins increased from 3.7–7.7 to 26–43% while modelled suspended sediment exports increased from 0.5–15 to 1.4–37 kt y^{-1}. Slow compartment residence times decreased because there was negligible change to the modelled atmospheric flux (F_aS_s) or ^{137}Cs inventory (M) and increased fluvial export associated with increased suspended sediment output. This corresponds to an increase in the radionuclide transport rate out of the slow compartment (k_s) that results in a decrease in the residence time (i.e. $\tau_s = 1/k_s$).

Slow compartment residence times cannot represent deeply eroded sediment from channel banks (i.e. sediment from below the depth of the ^{137}Cs inventory). This is because the model is unable to estimate the residence time of sediment that contains negligible levels of the fallout radionuclide tracers. Such sediment may come from deep colluvial or floodplain deposits that have not been exposed to fallout for long periods and where initial radionuclide activity has decayed to negligible levels. Therefore, the residence time estimates do not apply to particles stored in and subsequently eroded from these deposits.

Combining the modelled hillslope erosion rates with the slow compartment residence times produced an estimate of soil denudation depths. This was calculated using the mean RUSLE-derived hillslope erosion rate for the entire Tamar basin with the estimated *HSDR* of 0.15 to give net hillslope erosion rates for each land cover survey. The resulting range in mean denudation depths was 0.28–0.36 m, which equated to denudation rates of 11–39 mm ky^{-1}. These values were determined using a mean area-weighted soil bulk density of 0.9 t m^{-3}. This was calculated from spatially-distributed particle size and organic matter data for upper surface soils (mean maximum depth 0.23 m) in the Tamar basin using the method of Rawls (1983). The range in denudation depths was consistent with the depth of the upper soil profile containing the ^{137}Cs inventory (~0.3 m).

The slow compartment residence times were related to a basin-scale index of sediment transport capacity to support a physical interpretation of model outputs. This index was based on the representation of sediment transport capacity (q_s) as a function of discharge per unit slope width (q) and surface gradient as an approximation for energy slope (S), where $q_s = kq^{\beta}S^{\gamma}$, and k, β and γ are empirical or theoretically derived constants (Prosser and Rustomji, 2000). At the basin scale, modelled mean annual discharge per unit basin area was multiplied by the energy gradient approximated by basin slope using the relief ratio (RR), while the constants were set to 1.0. Both variables were normalized by their respective maximum values to produce a new index (MAD.RR) that varied between 0 and 1 (Table III).

Slow compartment residence time varied as a negative power function of MAD.RR for each land cover survey (Figure 3). The fitted power functions exhibited R^2 values ranging between 0.69 and 0.84 ($P < 0.05$). As sediment transport capacity (MAD.RR) approaches zero the slow compartment residence time goes to infinity, whereas at MAD.RR = 1 the coefficient equates to the minimum residence time associated with each land cover for the set of basins analysed. These minimum values were 13044, 6162 and 5392 years for the 1990, 2000 and 2007 land cover surveys, respectively. The decrease in the value of the coefficient and increase in the exponent captured the increase in basin-scale erodibility with increasing arable land area. With the increase in sediment available for transport, the range in slow compartment residence times associated with each function declined from 35 000 to 8400 years as sediment supply approaches basin-scale transport capacity. A theoretical minimum slow compartment residence time for each river basin would occur when sediment supply reached transport capacity assuming steady state conditions.

Mean residence times for the rapid transport compartment were 185–256, 243–362 and 260–368 days for the 1990, 2000 and 2007 surveys, respectively (Table V). The modelled area of the rapid transport compartment (S_r) also increased from 0.2–0.6 to 1.0–2.5% between 1990 and 2007. The modelled rapid transport area is dependent on the river output of ^{7}Be relative to atmospheric input to the rapid compartment (i.e. F_r/F_a) based on the assumption of negligible ^{7}Be input from the slow compartment compared with direct atmospheric input to the rapid compartment. Hancock *et al.* (2013) estimated that direct fallout of ^{7}Be onto wetted channels was insignificant compared with ^{7}Be exported with suspended sediment during a flow event for two large catchments in north-east Australia. This suggests most ^{7}Be associated with suspended sediment may be derived from connected source areas outside the channel network. Furthermore, the rapid transport compartment is unlikely to capture the contribution from channel bank erosion because sediment contributed by banks tends to contain negligible ^{7}Be (Wallbrink and Murray, 1993; Hancock *et al.*, 2013).

The increase in S_r related to the increase in F_r/F_a with consecutive land covers equated to an effective increase in the atmospheric input (F_aS_r) to the rapid compartment, which was proportionally larger than the increase in modelled ^{7}Be river

Table V. Modelled suspended sediment and fallout radionuclide (FRN) export and associated residence times for the slow (upper surface soils) and rapid (river and connected hillslope source area) compartments for the seven river basins and three land cover surveys

River basin/ survey year	Arable land area (%)	Modelled suspended sediment export (kt y^{-1})	Modelled FRN export, F_r (MBq y^{-1})[a]			Modelled particle residence times		Rapid compartment area, S_r (%)
			^{7}Be (× 10^2)	$^{210}Pb_{ex}$ (× 10^2)	^{137}Cs (× 10^2)	Slow, τ_s *upper soil profile* (ky)	Rapid, τ_r *river and connected area* (d)	
1990								
Tamar Upper	7.0	3.0	3.9	0.90	0.16	43	185	0.2
Ottery	6.1	1.5	2.0	0.48	0.08	48	204	0.2
Carey	6.6	0.9	1.0	0.30	0.06	33	256	0.3
Kensey	5.6	0.5	1.5	0.39	0.05	22	248	0.6
Lyd	7.7	4.7	7.4	2.3	0.52	13	241	0.5
Inny	3.7	1.2	2.8	0.75	0.13	26	231	0.4
Tamar Gunnislake	6.3	15	25	5.7	1.0	27	188	0.4
2000								
Tamar Upper	25	5.6	8.4	2.2	0.33	21	244	0.6
Ottery	27	3.9	6.0	1.8	0.22	17	297	0.9
Carey	21	1.5	2.0	0.67	0.11	17	322	0.7
Kensey	22	1.3	3.9	1.3	0.13	8.6	362	2.3
Lyd	14	7.0	12	4.1	0.86	7.7	280	1.0
Inny	17	2.7	7.3	2.5	0.31	10	344	1.4
Tamar Gunnislake	22	29	56	15	2.3	12	243	1.0
2007								
Tamar Upper	43	8.3	13	3.6	0.49	14	273	1.0
Ottery	43	5.2	8.1	2.5	0.29	12	317	1.3
Carey	37	2.1	2.9	1.0	0.15	12	357	1.0
Kensey	33	1.4	4.3	1.5	0.15	7.8	368	2.5
Lyd	29	9.7	17	6.0	1.2	5.6	307	1.5
Inny	26	3.0	8.1	2.8	0.35	9.2	358	1.6
Tamar Gunnislake	36	37	73	20	3.0	9.2	260	1.4

[a]Modelled FRN export (F_r) combined suspended sediment-associated FRN export with the estimated dissolved flux calculated using regionalized annual flow and partition coefficients (K_d) for each radionuclide.

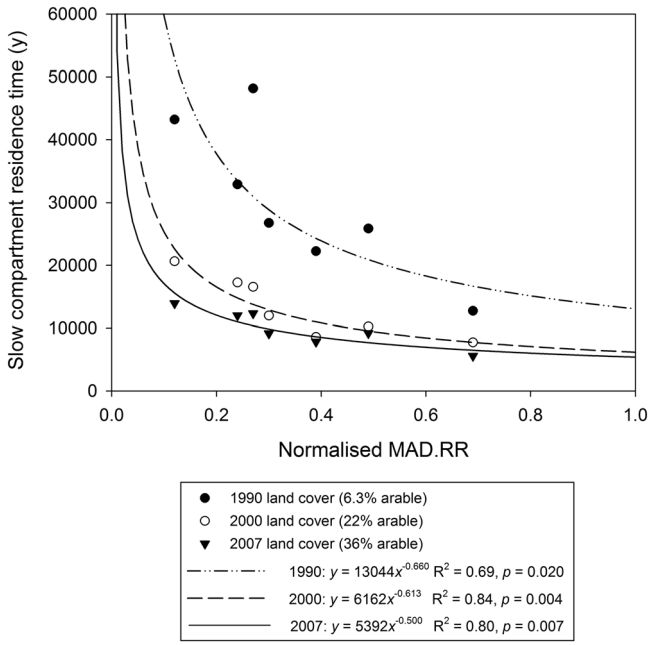

Figure 3. Slow compartment residence time versus the MAD.RR (Mean Annual Discharge multiplied by Relief Ratio) index (see text for details) for each river basin for the 1990, 2000 and 2007 land covers.

output (F_r). This led to an increase in the ^{7}Be inventory (I_r) of the rapid compartment. Therefore, the rapid compartment transport rate ($k_r = F_r/I_r$) decreased and the residence times ($\tau_r = 1/k_r$) increased with consecutive land cover surveys.

Model estimates of rapid compartment residence times assume that the duration of sediment storage will not result in net decay of ^{7}Be to levels below the limit of detection. In the Tamar basin, detectable levels of ^{7}Be were measured in suspended sediment samples collected using the time-integrated samplers over monthly intervals. The duration of in-channel storage of fine sediment would be unlikely to reduce ^{7}Be activity concentrations to negligible levels due to the frequency of flushing flows. Also fine sediment stored in-channel should not accumulate significant amounts of unattached $^{210}Pb_{ex}$. This has previously been used as a measure of in-channel residence time where storage times span a minimum of several years up to decades (Wallbrink *et al.*, 2002). The monthly suspended sediment samples collected over a 12 month period were assumed to capture the variability associated with ^{7}Be accumulation and decay in surface soils. This variability was reflected in the coefficient of variation for ^{7}Be activity concentrations on suspended sediment, which ranged between 28 and 58%.

The increase in S_r may be considered to reflect the expansion of connected near-channel source areas with increasing sediment supply. This is consistent with an increase in the area of arable land intersecting with the channel network that could supply more sediment. In the modelled scenarios for the Tamar basin, this equated to 0.6, 2.9 and 4.1 km^2 of riparian arable land within an arbitrarily defined 25 m buffer surrounding the modelled channel network for 1990, 2000 and 2007, respectively. The increase in rapid compartment residence times may also be interpreted in the context of the increase in S_r. Larger source areas are likely to correspond to longer sediment travel distances and hence increased residence times.

Temporary sediment storage on-slope is important for understanding timescales associated with hillslope sediment delivery processes. Particles move by a series of transport steps that may not scale with slope length (Parsons *et al.*, 2006). Runoff ratios tend to decline with increasing slope length (Sheridan *et al.*, 2013), which also contributes to increased particle residence times on longer slopes. Owing to the frequency of higher magnitude flows in the river network, the storage duration for most fine sediment within channels is probably short. Therefore, rapid compartment residence times may be largely associated with the number of runoff events required to deliver a particle to the channel network and the duration of particle storage between runoff events within connected slope source areas. The increase in rapid compartment residence times related to the expansion of connected source areas is conceptually linked to the increase in near-channel arable land that generates more sediment for transport.

Model evaluation and sensitivity

Sediment budgets

Modelled sediment budget components were examined in relation to available regional datasets in the absence of basin-specific validation data. The components considered were divided according to budget inputs that included RUSLE hillslope erosion rates, the hillslope sediment delivery ratio (*HSDR*) and channel bank erosion, and budget outputs, namely floodplain storage and basin-scale suspended sediment exports.

Mean RUSLE hillslope erosion rates calculated at the grid scale for forest, arable areas and grassland were 0.05–0.07, 6.0–6.8 and 0.29–0.31 t ha^{-1} y^{-1}, respectively. These erosion rates represent the range in mean values for each land cover recorded at the basin-scale for the three cover simulations. Combined, the three land cover types equate to 95–98% of the Tamar basin area. Therefore, the mean erosion rates capture the spatial variation in rainfall erosivity, soil erodibility, slope contributing area and gradient for the three land cover types across the basin. Model performance was assessed against regional datasets as well as a large-scale compilation of European erosion plot data.

Modelled mean erosion rates were generally consistent with published data. At the local scale, monitoring (1 year) in a small first-order grassland basin (0.46 km^2) located in Devon produced an estimated net erosion rate between 0.5 and1.2 t ha^{-1} y^{-1} for clayey soils (Bilotta *et al.*, 2010). These rates exceed long-term (11 years) plot-scale measurements for sandy soils under grass cover in central England, which gave a mean of 0.23 and range 0.1–0.5 t ha^{-1} y^{-1} (Fullen, 1998). Measurements in cultivated and pasture fields with clay-loam soils in south Devon using ^{137}Cs indicated erosion rates of 8.0 and 0.16 t ha^{-1} y^{-1}, respectively (Owens *et al.*, 1997). Furthermore, erosion rates estimated using ^{137}Cs for arable and pasture fields were 1.2–8.5 and 0.2–5.3 t ha^{-1} y^{-1}, respectively, in two small lowland basins (Walling *et al.*, 2002). However, comparison between modelled erosion rates and those measured using ^{137}Cs was limited by (i) difficulty in directly relating field-scale erosion measured using ^{137}Cs to soil loss estimates for slope segments based on RUSLE and (ii) untested assumptions in the use of ^{137}Cs to measure soil erosion that could produce erroneous results (Parsons and Foster, 2011). Analysis of a compilation of erosion plot data from across Europe that excluded the Mediterranean zone produced mean forest, cultivated and grassland erosion rates of 0.003, 6.3 and 0.29 t ha^{-1} y^{-1}, respectively (Cerdan *et al.*, 2010). The modelled arable and grassland erosion rates are consistent with this plot data. The much lower forest erosion rate was based on only 60 plot-months of data compared with 6635 and 1535 plot-months for cultivated and grassland plots (Cerdan *et al.*, 2010).

The modelled suspended sediment budgets were highly sensitive to change in the *HSDR*. An increase in *HSDR* from 0.05 to 0.15 corresponded to an approximately 3-fold increase in the basin-wide hillslope sediment contributions and a 1.5–2-

fold increase in the basin suspended sediment exports (Table III). The *HSDR* of 0.15 was selected on the basis of the detailed sediment budgets developed by Walling *et al.* (2002) for two small basins in central England (<4 km^2). These budgets measured in-field and field-to-channel deposition relative to gross erosion estimated using ^{137}Cs. While subject to the aforementioned uncertainties in the use of ^{137}Cs to measure soil erosion, these *HSDR* values provide the only available estimates of hillslope-to-channel sediment delivery in comparable agricultural basins and at a spatial scale equivalent to that of the individual river link drainage areas (mean ± SD = 9.96 ± 7.7 km^2) used in SedNet modelling of the Tamar basin. The *HSDR* of 0.15 was also chosen with reference to the resulting basin suspended sediment yields, which were consistent with regional yield estimates, as shown below.

Modelled link-average bank erosion rates ranged between 0 and 0.19 m y^{-1} (mean = 0.02 m y^{-1}) based on a coefficient value set to 0.0001 (Equation (2)) to limit the maximum rate of bank retreat (Wilkinson *et al.*, 2004). These bank retreat rates are in the low range of mean rates (0.03–1.18 m y^{-1}) from field measurements (1–3 y) for streams and rivers with basin areas ranging from 4.8–620 km^2 in south-west England (Hooke, 1980; Murgatroyd and Ternan, 1983). Longer-term (1840–1975) bank retreat rates measured from historic maps ranged from 0–1.79 m y^{-1} (Hooke, 1980). However, the comparatively low modelled bank erosion rates may be reasonable for several reasons. First, bank monitoring locations in the study by Hooke (1980) were biased towards areas of likely maximum erosion, particularly open floodplain sites. In contrast, the modelled channels have mean riparian forest cover ranging over 26–33% of the length of river links, thereby reducing bank retreat rates. Second, channel network confinement by bedrock and steep hillslopes occurs in many locations across the Tamar basin and limits lateral channel change. Third, low bank retreats rates are consistent with the preservation of small areas of floodplain in the Tamar basin. The modelled floodplain occupies 2.8% of the total basin area and has a mean width of only 70 ± 62 m. The largest area of floodplain occurs in the mid-basin where four tributaries join the main channel (Figure 1(b)). This represents productive agricultural land and hence bank stabilization measures have been adopted in some locations. It should be noted that modelled floodplain storage inputs do not offset channel bank losses (Table III). This should not be interpreted to imply a net loss from floodplain units. Channel bank erosion includes contributions from non-floodplain areas such as colluvial footslopes, while floodplains also receive inputs from adjacent hillslopes. No explicit calculation of hillslope-derived sediment inputs to floodplain storage units is made by the SedNet model.

Modelled floodplain deposition rates were low. Mean (and maximum) deposition rates for the 1990, 2000 and 2007 land covers were 0.04 (0.1), 0.08 (0.2) and 0.12 (0.3) mm y^{-1}, respectively. Measurement of floodplain deposition rates using ^{137}Cs in five river basins (276–3717 km^2) in southern England yielded a range in mean reach-scale values of 0.7–1.6 mm y^{-1} since the mid-1950s (Walling and He, 1998). Inundation of these floodplain reaches was estimated to occur several times per year. In another study set in northern England, the mean sedimentation rates for floodplain transects extending from the channel margin to the outer floodplain were 0.07–3.7 and 0.1–1.5 mm y^{-1} for the River Ouse and River Tweed, respectively (Walling *et al.*, 1999). These rates were converted from g cm^{-2} y^{-1} to mm y^{-1} using a sediment bulk density of 1.5 g cm^{-3}. The lower modelled floodplain deposition rates probably result in part from the effect of averaging annual overbank sediment deposition across the entire modelled floodplain area for each river link. Floodplain deposition is not spatially uniform, as shown by declining sedimentation rates with distance from channels (Walling *et al.*, 1999). The comparison with mean rates for transects spanning most of the floodplain reduces this disparity. Floodplain inundation frequency is also an important factor distinguishing sedimentation rates. SedNet simulations used a basin-wide bankfull discharge frequency of 1.5 years on the annual series to determine the proportion of overbank flow. Inundation frequency will be higher in some near-channel locations, as was the case for floodplain reaches measured by Walling and He (1998).

Modelled suspended sediment yields for the Tamar basin at Gunnislake were 16–40 t km^{-2} y^{-1} using an *HSDR* of 0.15 for the three land covers. This range in yields is comparable with suspended sediment yields obtained from longer-term (1994–2003) monitoring of three agricultural river basins (226–601 km^2) in Devon (Harlow *et al.*, 2006). These measured yields range from 24 to 45 t km^{-2} y^{-1}, and provide a good comparison with modelled yields on the basis of general similarities in basin land use and hydroclimatic conditions. Such longer-term measurements of yield are preferable for use in assessing model performance given that SedNet computes mean annual budgets over a timescale of several decades. The modelled yields were also consistent with an earlier regional compilation of river basin suspended sediment yields from south-west England (Walling and Webb, 1987). In this compilation, the range in suspended sediment yields was 16–58 t km^{-2} y^{-1} for basins with areas ranging between 46 and 422 km^2, excluding the three basins with more recent data reported by Harlow *et al.* (2006) and those basins <10 km^2. This is also consistent with the modelled suspended sediment yields for the Tamar sub-basins (38–238 km^2) which ranged from 12–21, 22–34 and 31–44 t km^{-2} y^{-1} for the 1990, 2000 and 2007 land covers, respectively. Notably, the range in modelled yields spanning the three land cover surveys is consistent with the range in measured yields. This indicates that the effect of land use change on modelled yields in the Tamar basin does not exceed regional variability in mean annual suspended sediment yields.

Particle residence times

The performance of the particle residence time model cannot be examined directly due to (i) the absence of independent validation datasets and (ii) the difficulty in validating estimates of slow compartment residence times for specific land covers that do not change through time. Instead we use a sensitivity analysis to identify those parameters which exert greater influence on model outputs and compare estimates of parameter values with available measurements.

The sensitivity analysis showed that a factor change of 0.5 and 1.5 to individual model parameters could result in factor changes to slow and rapid compartment residence times ranging between 0.4 and 2.6 (Table VI). However, most changes in residence time estimates remained within the range 0.5–1.5. Slow compartment residence time was most sensitive to changes in suspended sediment flux and basin-scale ^{137}Cs inventory (M), whereas the rapid compartment residence time and S_r were most sensitive to changes in F_a ($^{210}Pb_{ex}$). Changes to F_a (^{7}Be) affected only the rapid compartment residence time. Slow compartment residence times were unaffected by changes in F_a for ^{7}Be or $^{210}Pb_{ex}$. Ignoring the partitioning of the radionuclides between the dissolved and particulate forms (i.e. $K_d \rightarrow \infty$) increased model estimates of S_r, slow and rapid compartment residence times, by factors of 1.0–1.3 (Table VI). This was equivalent to the effect of increasing F_a (^{7}Be) or M, with a negligible effect for F_a ($^{210}Pb_{ex}$) due to its already high K_d (Le Cloarec *et al.*, 2007).

The sensitivity analysis indicated that the estimates of suspended sediment flux, M and F_a for ^{7}Be and $^{210}Pb_{ex}$ exert an important control on model outputs. Modelled mean annual

Table VI. Summary of factor changes in τ_s, τ_r and S_r in response to changes in residence time model parameters for the Tamar basin upstream of Gunnislake under the 2007 land cover

Model input	Factor change in parameter values	Factor changes in model outputs		
		Slow compartment (τ_s)	Rapid compartment (τ_r)	Rapid compartment area (S_r)
Suspended sediment flux	1.5	0.7	1.1	1.5
	0.5	1.7	0.8	0.5
	Increase parameter	Decrease	Increase	Increase
Radionuclide activity concentration[a]	+ 2SE	0.9	1.0	1.1
	– 2SE	1.1	1.0	0.9
	Increase parameter	Decrease	Negligible change	Increase
F_a ($^{210}Pb_{ex}$)	1.5	1.0	0.5	0.6
	0.5	1.0	2.6	2.3
	Increase parameter	Negligible change	Decrease	Decrease
F_a (^{7}Be)	1.5	1.0	1.6	1.0
	0.5	1.0	0.4	1.0
	Increase parameter	Negligible change	Increase	Negligible change
M (^{137}Cs)	1.5	1.5	1.1	1.1
	0.5	0.5	0.7	0.8
	Increase parameter	Increase	Increase	Increase
Ignore K_d		1.2	1.3	1.0
Most sensitive parameters		*SS* and *M*	F_a ($^{210}Pb_{ex}$)	F_a ($^{210}Pb_{ex}$)

[a]Radionuclide activity concentrations were varied by ±2 standard errors (SE) reported in Table III.

suspended sediment yields were shown to be comparable with longer-term measurements from agricultural river basins in the region. Uncertainty in the measured mean radionuclide activity concentrations (Table III) used in calculating F_r was constrained by the use of continuous time-integrated sampling that captured a range of flow conditions over a 12 month period. Varying these activity concentrations by ±2 standard errors had only a minor effect on model outputs (Table VI). However, the necessary scaling of activity concentrations to reflect changes in modelled hillslope and channel bank sediment contributions introduced additional uncertainty in residence time estimates. Decreasing the estimated suspended sediment activity concentrations for the 1990 and 2000 land cover simulations was consistent with lower modelled sediment contributions from hillslope surface erosion. M was estimated for each river basin using the relationship between soil ^{137}Cs inventory and mean annual rainfall derived by Appleby *et al.* (2003) with the 1 × 1 km gridded 1971–2000 precipitation data. This produced a range in areal ^{137}Cs inventories of 2820–3390 Bq m^{-2}. This approach captured the spatial variability associated with precipitation patterns. Higher inventories occurred across elevated areas of the Tamar basin in the east and west compared with lower inventories in the centre and northern part of the basin.

Possibly the largest source of uncertainty in model inputs relates to the estimates of F_a for ^{7}Be and $^{210}Pb_{ex}$. The range in areal fallout values used to derive F_a for ^{7}Be was 2330–2930 Bq m^{-2} y^{-1} (mean precipitation = 1180–1488 mm y^{-1}). This was consistent with measurements of 2750 (Dominik *et al.*, 1987) and 2670 Bq m^{-2} y^{-1} (Schuler *et al.*, 1991) in Switzerland for precipitation of 1100–1200 mm y^{-1} which is comparable with the study basins. However, it is higher than 1618 Bq m^{-2} y^{-1} (precipitation = 1328 mm y^{-1}) at Milford Haven in south Wales (Peirson *et al.*, 1966) and 1200 Bq m^{-2} y^{-1} (precipitation not reported) for the Seine River basin (Le Cloarec *et al.*, 2007), but lower than 3912 ± 120 Bq m^{-2} y^{-1} (precipitation = 1884 mm y^{-1}) in Cumbria, northern England (Short *et al.*, 2007). In addition to annual rainfall amount and latitude, solar activity is an important control of ^{7}Be production, which varies by ~25% with the 11 year solar cycle (Kaste *et al.*, 2002). Therefore, differences between studies may in part reflect solar variability. Variation in F_a (^{7}Be) affects only the rapid compartment residence times (Table VI). The large range in reported annual atmospheric fallout and the effect of solar variability indicates that rapid compartment residence times are probably subject to greater uncertainty than slow compartment residence times which are unaffected by variation in F_a (^{7}Be). However, it can be anticipated that this uncertainty was reduced to some extent by the use of 30 year mean annual precipitation data to compute ^{7}Be fallout.

The range in estimated mean areal fallout values used to derive F_a for $^{210}Pb_{ex}$ was 118–149 Bq m^{-2} y^{-1}. These values were less than 165 ± 8 Bq m^{-2} y^{-1} based on measurements of $^{210}Pb_{ex}$ concentration in rainwater for 1997–1998 in Cumbria (Short *et al.*, 2007). However, this is consistent with higher mean annual rainfall (1884 mm) for the Cumbrian site as well as the proximity of the Tamar study basin to the east coast of the Atlantic (i.e. air mass with reduced geogenic ^{222}Rn activity). The range in $^{210}Pb_{ex}$ atmospheric flux in the present study lies between the mean of 117 Bq m^{-2} y^{-1} estimated for the 30–60° N latitude zone based on a compilation of data (Preiss *et al.*, 1996) and 161 Bq m^{-2} y^{-1} from soil inventories in Devon (Walling and He, 1999). These comparisons suggest that estimates of F_a for $^{210}Pb_{ex}$ were reasonable.

Conclusions

This is the first study to combine a sediment residence time model with multi-decadal estimates of mean annual discharge and suspended sediment export from river basins. In contrast, previous applications have been based on short-term monitoring (1–2 years) that is highly dependent on the specific hydroclimatic conditions during measurement periods. This may have an important effect on estimated residence times due to model sensitivity to suspended sediment exports. The novel combination of a river basin sediment budget model with a mass balance model of particle residence times that uses fallout radionuclide tracers identified changes in spatial patterns and timescales of suspended sediment transfer in response to recent agricultural land cover change. With increased pressure on soil systems to meet global food security targets, such information is highly valuable to catchment managers and policy makers who need to balance food production against protection of downstream water resources and aquatic ecosystems.

The SedNet model was used to simulate mean annual suspended sediment fluxes for three land cover surveys spanning a period of recent change in agricultural land use in the study basin. Modelled basin-scale suspended sediment yields ranged between 16 and 40 t km^{-2} y^{-1} and were consistent with longer-term measurements from the region. Likewise, hillslope and channel bank erosion rates were comparable to available data suggesting that the SedNet model provided a reasonable representation of suspended sediment transfer. Comparison of modelled sediment budgets between land cover surveys showed a pronounced increase in suspended sediment yields in response to an increase in the area of arable land from 6.3 to 36% between 1990 and 2007.

Modelled particle residence times were estimated for seven sub-basins that were divided into slow (upper surface soil) and rapid (river and connected hillslope source areas) transport compartments. Modelled slow compartment residence times for the river basins were 13–48, 7.7–17 and 5.6–14 ky for the 1990, 2000 and 2007 land cover surveys, respectively. The residence times decreased in response to the increase in modelled suspended sediment exports with increasing arable land area. It was also shown that slow compartment residence times were related to a basin-scale index of sediment transport capacity by a negative power function for each land cover. Both the residence times and estimated source areas of the rapid transport compartment increased with consecutive land cover surveys. Conceptually, this was considered to reflect the expansion of connected hillslope source areas with increasing sediment supply from more arable land situated near the channel network. Larger source areas correspond to longer sediment travel distances and hence increased residence times.

The coupled sediment budget-residence time modelling approach provides unique insight into river basin responses to recent environmental change not otherwise available from conventional measurement techniques. Quantifying residence times of fine sediment and associated contaminants in degraded river basins may yield valuable information on potential recovery rates from pollution under current environmental conditions. Future environmental changes could also be modelled. For example, the use of a sediment budget model with hydrologic parameters such as SedNet would allow examination of the potential impact on sediment residence times of projected changes in precipitation and evaporation associated with future climate scenarios.

Acknowledgements—HGS acknowledges the support of a Marie Curie Fellowship (PIIF-GA-2010-273069) within the 7th European Community Framework Programme. This paper also represents a contribution to the International Atomic Energy Agency Coordinated Research Programme D1.20.11 under Research Agreement IAEA contract UK/15538 (WB). We thank staff from the Westcountry Rivers Trust for help with site selection and arranging access for river monitoring. We also acknowledge the contribution of Professor Geoff Millward to gamma spectrometry analysis and for lively discussion. We thank two anonymous reviewers whose comments helped improve the manuscript.

References

Abernethy B, Rutherfurd ID. 2001. The distribution and strength of riparian tree roots in relation to riverbank reinforcement. *Hydrological Processes* **15**: 63–79.

Appleby PG, Haworth EY, Michel H, Short DB, Laptev G, Piliposian GT. 2003. The transport and mass balance of fallout radionuclides in Blelham Tarn, Cumbria (UK). *Journal of Paleolimnology* **29**: 459–473.

Bilotta GS, Krueger T, Brazier RE, Butler P, Freer J, Hawkins JMB, Haygarth PM, Macleod CJA, Quinton JN. 2010. Assessing catchment-scale erosion and yields of suspended solids from improved temperate grassland. *Journal of Environmental Monitoring* **12**: 731–739.

Bonniwell EC, Matisoff G, Whioting PJ. 1999. Determining the times and distances of particle transit in a mountain stream using fallout radionuclides. *Geomorphology* **27**: 75–92.

Brune GM. 1953. Trap efficiency of reservoirs. *Transactions of the American Geophysical Union* **34**: 407–418

Cawse PA. 1983. The accumulation of ^{137}Cs and $^{239+240}$Pu in soils of Great Britain, and transfer to vegetation. In Ecological Aspects of Radionuclide Release, Coughtrey PJ (eds). Blackwell: Oxford; 47–62.

Cerdan O, Govers G, Le Bissonnais Y, Van Oost K, Poesen J, Saby N, Gobin A, Vacca A, Quinton J, Auerswald K, Klik A, Kwaad FJPM, Raclot D, Ionita I, Rejman J, Rousseva S, Muxart T, Roxo MJ, Dostal T. 2010. Rates and spatial variations of soil erosion in Europe: a study based on erosion plot data. *Geomorphology* **122**: 167–177.

Coulthard TJ, Macklin MG. 2003. Modeling long-term contamination in river systems from historical metal mining. *Geology* **31**: 451–454.

Cremers A, Elson A, De Preter P, Maes A. 1988. Quantitative analysis of radiocaesium retention in soils. *Nature* **335**: 247–249.

Davidson SK, Hey RD. 2011. Regime equations for natural meandering cobble- and gravel-bed rivers. *Journal of Hydraulic Engineering* **137**: 894–910.

Department of Environment, Food and Rural Affairs (DEFRA). 2010. Structure of the agricultural industry in England and the UK at June. https://www.gov.uk/government/statistical-data-sets/structure-of-the-agricultural-industry-in-england-and-the-uk-at-june

Desmet PJJ, Govers G. 1996. A GIS procedure for automatically calculating the USLE LS factor of topographically complex landscape units. *Journal of Soil and Water Conservation* **51**: 427–433.

Dietrich WE, Dunne T. 1978. Sediment budget for a small catchment in mountainous terrain. *Zeitschrift für Geomorphologie* **29**: 191–206.

Dominik J, Burrus D, Vernet J-P. 1987. Transport of environmental radionuclides in an alpine watershed. *Earth and Planetary Science Letters* **84**: 165–180.

Dosseto D, Hesse PP, Maher K, Fryirs K, Turner S. 2010. Climatic and vegetation control on sediment dynamics during the last glacial cycle. *Geology* **38**: 395–398.

Evrard O, Némery J, Gratiot N, Duvert C, Ayrault S, Lefèvre I, Poulenard J, Prat C, Bonté P, Esteves M. 2010. Sediment dynamics during the rainy season in tropical highland catchments of central Mexico using fallout radionuclides. *Geomorphology* **124**: 42–54.

Fifield LK, Wasson RJ, Pillans B, Stone JOH. 2010. The longevity of hillslope soil in SE and NW Australia. *Catena* **81**: 32–42.

Fryirs K. 2013. (Dis)Connectivity in catchment sediment cascades: a fresh look at the sediment delivery problem. *Earth Surface Processes and Landforms* **38**: 30–46.

Fu G, Chen S, McCool DK. 2006. Modeling the impacts of no-till practice on soil erosion and sediment yield with RUSLE, SEDD and ArcView GIS. *Soil and Tillage Research* **85**: 38–49.

Fullen MA. 1998. Effects of grass ley set-aside on runoff, erosion and organic matter levels in sandy soils in east Shopshire, UK. *Soil and Tillage Research* **46**: 41–49.

Fuller RM, Smith GM, Devereux BJ. 2003. The characterisation and measurement of land cover change through remote sensing: problems in operational applications? *International Journal of Applied Earth Observation and Geoinformation* **4**: 243–253.

Gallant JC, Dowling TI. 2003. A multiresolution index of valley bottom flatness for mapping depositional areas. *Water Resources Research* **39**: 1347.

Gartner JD, Renshaw CE, Dade WB, Magilligan FJ. 2012. Time and depth scales of fine sediment delivery into gravel stream beds: constraints from fallout radionuclides on fine sediment residence time and delivery. *Geomorphology* **151–152**: 39–49.

Granet M, Chabaux F, Stille P, Dosseto A, France-Lanord C, Blaes E. 2010. U-series disequilibria in suspended river sediments and implication for sediment transfer time in alluvial plains: the case of the Himalayam rivers. *Geochemica et Cosmochimica Acta* **74**: 2851–2865.

Hancock GJ, Wilkinson SN, Hawdon AA, Keen RJ. 2013. Use of fallout tracers ^{7}Be, ^{210}Pb and ^{137}Cs to distinguish the form of sub-surface soil erosion delivering sediment to rivers in large catchments. *Hydrological Processes*. DOI: 10.1002/hyp.9926

Harlow A, Webb B, Walling D. 2006. Sediment yields in the Exe basin: a longer-term perspective. In Sediment Dynamics and the

Hydromorphology of Fluvial Systems, Rowna JS, Duck RW, Werritty A (eds). International Association of Hydrological Sciences Publ. No. 306: Wallingford; 12–20.

He Q, Walling DE. 1996. Interpreting particle size effects in the adsorption of ^{137}Cs and unsupported ^{210}Pb by minerals soils and sediments. *Journal of Environmental Radioactivity* **30**: 117–137.

Heimsath AM, Chappell J, Dietrich WE, Nishiizumi K, Finkel RC. 2001. Late Quaternary erosion in southeastern Australia: a field example using cosmogenic nuclides. *Quaternary International* **83–85**: 169–185.

Heinemann HG. 1981. A new sediment trap efficiency curve for small reservoirs. *Water Resources Bulletin* **17**: 825–830.

Hooke JM. 1980. Magnitude and distribution of rates of river bank erosion. *Earth Surface Processes* **5**: 143–157.

Hughes AO, Croke JC. 2011. Validation of a spatially distributed erosion and sediment yield model (SedNet) with empirically derived data from a catchment adjacent to the Great Barrier Reef Lagoon. *Marine and Freshwater Research* **62**: 962–973.

Kaste JM, Norton SA, Hess CT. 2002. Environmental chemistry of beryllium-7. In Beryllium: Mineralogy, Petrology and Geochemistry, Grew ES (ed). Washington Mineralogical Society America: 271–289.

Kelsey HM, Lamberson R, Madej MA. 1987. Stochastic model for the long-term transport of stored sediment in a river channel. *Water Resources Research* **23**: 1738–1750.

Le Cloarec M-F, Bonté P, Lefèvre I, Mouchel J-M, Colbert S. 2007. Distribution of ^{7}Be, ^{210}Pb and ^{137}Cs in watersheds of difference scales in the Seine River basin: inventories and residence times. *Science of the Total Environment* **375**: 125–139.

Mabit L, Benmansour M, Walling DE. 2008. Comparative advantages and limitations of the fallout radionuclides ^{137}Cs, ^{210}Pb$_{ex}$ and ^{7}Be for assessing soil erosion and sedimentation. *Journal of Environmental Radioactivity* **99**: 1799–1807.

Malmon DV Dunne T, Reneau SL. 2003. Stochastic theory of particle trajectories through alluvial valley floors. *The Journal of Geology* **111**: 525–542.

Malmon DV, Reneau SL, Dunne T, Katzman D, Drakos PG. 2005. Influence of sediment storage on downstream delivery of contaminated sediment. *Water Resources Research* **41**: W05008

Marshall JS, Palmer WM. 1948. The distribution of raindrops with size. *Journal of Meteorology* **5**: 165–166.

Matisoff G, Wilson CG, Whiting PJ. 2005. The ^{7}Be/^{210}Pb$_{xs}$ ratio as an indicator of suspended sediment age or fraction new sediment in suspension. *Earth Surface Processes and Landforms* **30**: 1191–1201.

McCool DK, Brown LC, Foster GR, Mutchler CK, Meyer LD. 1987. Revised slope steepness factor for the universal soil loss equation. *Transactions of the Association of Agricultural Engineers* **30**: 1387–1396.

McKergow LA, Prosser IP, Hughes AO, Brodie J. 2005. Sources of sediment to the Great Barrier Reef World Heritage Area. *Marine Pollution Bulletin* **51**: 200–211.

Morgan RPC. 2001. A simple approach to soil loss prediction: a revised Morgan-Morgan-Finney model. *Catena* **44**: 305–322.

Morgan RPC. 2005. Soil Erosion and Conservation. Blackwell Publishing: Oxford.

Morton D, Rowland C, Wood C, Meek L, Marston C, Smith G, Simpson IC. 2011. Final report for LCM2007 – the new UK land cover map. CS Technical Report No 11/07 NERC/Centre for Ecology and Hydrology, Wallingford.

Murgatroyd AL, Ternan JL. 1983. The impact of afforestation on stream bank erosion and channel form. *Earth Surface Processes and Landforms* **8**: 357–369.

Owens PN, Walling DE, He Q, Shanahan J., Foster IDL. 1997. The use of caesium-137 measurements to establish a sediment budget for the Start catchment, Devon, UK. *Hydrological Sciences Journal* **42**: 405–423.

Parsons AJ, Foster IDL. 2011. What can we learn about soil erosion from the use of ^{137}Cs? *Earth-Science Reviews* **108**: 101–113.

Parsons AJ, Brazier RE, Wainwright J, Powell DM. 2006. Scale relationships in hillslope runoff and erosion. *Earth Surface Processes and Landforms* **31**: 1384–1393.

Peirson DH, Cambray RS, Spicer GS. 1966. Lead-210 and polonium-210 in the atmosphere. *Tellus* **18**: 427–433.

Phillips JM, Russell MA, Walling DE. 2000. Time-integrated sampling of fluvial suspended sediment: a simple methodology for small catchments. *Hydrological Processes* **14**: 2589–2602.

Preiss N, Mélières, M-A, Pourchet M. 1996. A compilation of data on lead 210 concentration in surface air and fluxes at the air-surface and water-sediment interfaces. *Journal of Geophysical Research* **101**: 28847–28862.

Prosser IP, Rustomji P. 2000. Sediment transport capacity relations for overland flow. *Progress in Physical Geography* **24**: 179–193.

Prosser IP, Rustomji P, Young B, Moran C, Hughes A. 2001a. Constructing river basin sediment budgets for the National Land and Water Resources Audit. CSIRO Land and Water Technical Report 15/01, Canberra.

Prosser IP, Rutherfurd ID, Olley JM, Young WJ, Wallbrink PJ, Moran CJ. 2001b. Large-scale patterns of erosion and sediment transport in river networks, with examples from Australia. *Marine and Freshwater Research* **52**: 81–99.

Rawls WJ. 1983. Estimating soil bulk density from particle size analysis and organic matter content. *Soil Science* **135**: 123–125.

Renard KG, Foster GR, Weesies GA, McCool DK, Yoder, DC. 1997. Predicting soil erosion by water: a guide to conservation planning with the Revised Universal Soil Loss Equation (RUSLE). United States Department of Agriculture Handbook No. 703.

Schuler C, Wieland E, Santschi PH, Sturm M, Lueck A, Bollhalder S, Beer J, Bonani G, Hofman HJ, Suter M, Wolfli W. 1991. A multitracer study of radionuclides in Lake Zurich, Switzerland 1. Comparison of atmospheric and sedimentary fluxes of ^{7}Be, ^{10}Be, ^{210}Pb, ^{210}Po and ^{137}Cs. *Journal of Geophysical Research* **96**: 17051–17065.

Sheridan GJ, Noske PJ, Lane PNJ, Jones OD, Sherwin CB. 2013. A simple two-parameter model for scaling hillslope surface runoff. *Earth Surface Processes and Landforms*. DOI: 10.1002/esp.3503

Short DB, Appleby PG, Hilton J. 2007. Measurement of atmospheric fluxes of radionuclides at a UK site using both direct (rain) and indirect (soils) methods. *International Journal of Environment and Pollution* **29**: 392–404.

Slattery MC, Gares PA, Phillips JD. 2002. Slope-channel linkage and sediment delivery on North Carolina coastal plain cropland. *Earth Surface Processes and Landforms* **27**: 1377–1387.

Smith HG, Sheridan GJ, Lane PNJ, Noske PJ, Heijnis H. 2011. Changes to sediment sources following wildfire in a forested upland catchment, southeastern Australia. *Hydrological Processes* **25**: 2878–2889.

Taylor A. 2012. The environmental behaviour of beryllium-7 and implications for its use as a sediment tracer. PhD thesis, Plymouth University.

Taylor A, Blake WH, Couldrick L, Keith-Roach MJ. 2012. Sorption behaviour of beryllium-7 and implications for its use as a sediment tracer. *Geoderma* **187–188**: 16–23.

Taylor A, Blake WH, Smith HG, Mabit L, Keith-Roach MJ. 2013. Assumptions and challenges in the use of fallout beryllium-7 as a soil and sediment tracer in river basins. *Earth-Science Reviews* DOI:10.1016/j.earscirev.2013.08.002

Thorne CR. 1990. Effects of vegetation on riverbank erosion and stability. In Vegetation and Erosion, Thornes JB (ed). John Wiley and Sons: Chichester; 125–144.

Van Rompaey AJJ, Govers G. 2002. Data quality and model complexity for regional scale soil erosion prediction. *International Journal of Geographical Information Science* **16**: 663–680.

Von Blanckenburg F 2005. The control mechanisms of erosion and weathering at basin scale from cosmogenic nuclides in river sediment. *Earth and Planetary Science Letters* **237**: 462–479.

Wallbrink PJ, Murray AS. 1993. Use of fallout radionuclides as indicators of erosion processes. *Hydrological Processes* **7**: 297–304.

Wallbrink PJ, Murray AS. 1994. Fallout ^{7}Be in south eastern Australia. *Journal of Environmental Radioactivity* **25**: 213–228.

Wallbrink PJ, Murray AS, Olley JM, Olive LJ. 1998. Determining sources and transit times of suspended sediment in the Murrumbidgee River, New South Wales, Australia, using fallout ^{137}Cs and ^{210}Pb. *Water Resources Research* **34**: 879–887.

Wallbrink PJ, Murray AS, Olley JM. 1999. Relating suspended sediment to its original soil depth using fallout radionuclides. *Soil Science Society of America Journal* **63**: 369–378.

Wallbrink PJ, Olley JM, Hancock G. 2002. Estimating residence times of fine sediment in river channels using fallout ^{210}Pb. In The Structure, Function and Management Implications of Fluvial Sedimentary Systems, Dyer FJ, Thoms MC, O JM (eds). International Association of Hydrological Sciences Publ. No 276: Wallingford; 425–432.

Wallbrink PJ, Martin CE, Wilson CJ. 2003. Quantifying the contributions of sediment, sediment-P and fertiliser-P from forested, cultivated and pasture areas at the landuse and catchment scale using fallout radionuclides and geochemistry. *Soil and Tillage Research* **69**: 53–68.

Walling DE. 2003. Using environmental radionuclides as tracers in sediment budget investigations. In: Erosion and Sediment Transport Measurement in Rivers: Technological and Methodological Advances, Bogen J, Fergus T, Walling DE (eds). International Association of Hydrological Sciences Publ. No. 283: Wallingford; 57–78.

Walling DE, He Q. 1998. The spatial variability of overbank sedimentation on river floodplains. *Geomorphology* **24**: 209–223.

Walling DE, He Q. 1999. Using fallout lead-210 measurements to estimate soil erosion on cultivated land. *Soil Science Society of America Journal* **63**: 1404–1412.

Walling DE, Webb BW. 1987. Suspended load in gravel bed rivers: UK experience. In Sediment Transport in Gravel-Bed Rivers, Thorne CR, Bathurst JC, Hey RD (eds). John Wiley and Sons: Chicester; 767–782.

Walling DE, Rowan JS, Bradley SB. 1989. Sediment-associated transport and redistribution of Chernobyl fallout radionuclides. In Sediment and the Environment, Hadley RF, Ongley ED (eds). International Association of Hydrological Sciences Publ. No. 184: Wallingford; 37–45.

Walling DE, Owens PN, Leeks GJL. 1999. Rates of contemporary overbank sedimentation and sediment storage on the floodplains of the main channel systems of the Yorkshire Ouse ad River Tweed, UK. *Hydrological Processes* **13**: 993–1009.

Walling DE, Russell MA, Hodgkinson RA, Zhang Y. 2002. Establishing sediment budgets for two small lowland agricultural catchments in the UK. *Catena* **47**: 323–353.

Wilkinson SN, Henderson A, Chen Y. 2004. SedNet user guide. CSIRO Land and Water: Canberra.

Wilkinson SN, Olley JM, Prosser IP, Read IP. 2005. Targeting erosion control in large river systems using spatially distributed sediment budgets. In Geomorphological Processes and Human Impacts in River Basins, Batalla RJ, Garcia C (eds). International Association of Hydrological Sciences Publ. No. 299: Wallingford; 56–64.

Wilkinson SN, Young WJ, DeRose RC. 2006. Regionalizing mean annual flow and daily flow variability for basin-scale sediment and nutrient modelling. *Hydrological Processes* **20**: 2769–2786.

Wilkinson SN, Prosser IP, Rustomji P, Read AM. 2009. Modelling and testing spatially distributed sediment budgets to relate erosion processes to sediment yield. *Environmental Modelling and Software* **24**: 489–501.

Wischmeier WH, Smith DD. 1978. Predicting rainfall erosion losses – a guide to conservation planning. United States Department of Agriculture Handbook No. 537.

Zhang L, Hickel K, Dawes WR, Chiew FHS, Western AW, Briggs PR. 2004. A rational function approach for estimating mean annual evapotranspiration. *Water Resources Research* **40**: W02502.

